

See discussions, stats, and author profiles for this publication at: <https://www.researchgate.net/publication/231633864>

Bound-Excited Electronic States of the Anion of 2,3,5,6-Tetrafluoro-7,7,8,8-tetracyanoquinodimethane†

ARTICLE *in* THE JOURNAL OF PHYSICAL CHEMISTRY A · APRIL 2003

Impact Factor: 2.69 · DOI: 10.1021/jp0222999

CITATIONS

15

READS

26

3 AUTHORS, INCLUDING:



Piotr Skurski

University of Gdansk

141 PUBLICATIONS 3,382 CITATIONS

SEE PROFILE

Bound-Excited Electronic States of the Anion of 2,3,5,6-Tetrafluoro-7,7,8,8-tetracyanoquinodimethane[†]

Monika Sobczyk,^{‡,§} Piotr Skurski,^{‡,§} and Jack Simons^{*,§}

Department of Chemistry, University of Gdansk, ul. Sobieskiego 18, 80–952 Gdansk, Poland, and Henry Eyring Center for Theoretical Chemistry, Department of Chemistry, University of Utah, Salt Lake City, Utah 84112

Received: October 23, 2002; In Final Form: February 11, 2003

The doublet anionic states of TCNQ-F4 (2,3,5,6-tetrafluoro-7,7,8,8-tetracyanoquinodimethane) have been studied at the Hartree–Fock and the Møller–Plesset (MP) perturbation theory levels (up to fourth order) with aug(sp)-pVDZ basis sets. Our results indicate that TCNQ-F4 forms a stable anion of B_{2g} symmetry whose vertical electron attachment energy is 2.893 eV (at the MP4 level). In addition, we found two valence excited electronic states (2^2B_{3u} and 1^2A_g) of the anion that are stable vertically with respect to the neutral parent. The electronic stability of the third excited state (a core-excited 1^2B_{3u} state) needs to be further investigated. We conclude that the neutral TCNQ-F4 at its equilibrium D_{2h} geometry may attach an excess electron to form any of these four states (i.e., 1^2B_{2g} , 1^2B_{3u} , 2^2B_{3u} , and 1^2A_g) and the corresponding MP4 vertical attachment energies (VAE) are 2.893, 0.822, 0.244, and 0.072 eV, respectively. However, due to second-order Jahn–Teller distortion, only the ground anionic state (1^2B_{2g}) possesses a minimum at D_{2h} symmetry. For the two valence excited states (2^2B_{3u} and 1^2A_g), negative curvatures cause out-of-plane deformations that lead to (i) an increase of the energy of the latter (1^2A_g) state and (ii) achieving a minimum-energy structure of C_2 symmetry for the former where this state becomes a doublet A state and its vertical electronic stability increases to 2.721 eV.

1. Introduction

Very few anions possess bound excited electronic states, and the systems characterized to date are primarily atoms or diatomics.^{1–3} In this contribution we study *valence* excited anionic states, in which an excess electron occupies a valence orbital of the neutral molecule, rather than dipole-bound anionic states, in which an extra electron is bound primarily due to the electrostatic interactions with the neutral molecule.^{4–9} In the 90s Simons and Gutowski studied lithium-substituted double-Rydberg anions that possess a few bound valence anionic states.^{10–12} These states, however, differ in multiplicity. In the present work, we address a molecular system with bound anionic states of the same spin multiplicity.

Brauman and co-workers observed bound valence excited anionic states of TCNQ (7,7,8,8-tetracyanoquinodimethane), TCNE (tetracyanoethylene), Me₂-DCNQI (2,5-dimethyl-*N,N'*-dicyanoquinodimine), chloranil, and hexacyanobutadiene in electron photodetachment spectroscopy experiments.^{13,14} The most extensive experimental results are available for TCNQ[–], a species that we studied in the past.¹⁵ On the basis of CI/PM3 calculations, we suggested that the $1^2B_{3u} \rightarrow 2^2B_{2g}$ and $2^2B_{3u} \rightarrow 2^2B_{2g}$ transitions contributed to the electronic absorption and electron photodetachment spectra of TCNQ[–].¹⁵ These results supported the experimental claim from the Brauman group that not only the ground anionic state (2^2B_{2g}) but also certain excited states of TCNQ[–] (i.e., 1^2B_{3u} and 2^2B_{3u}) were electronically

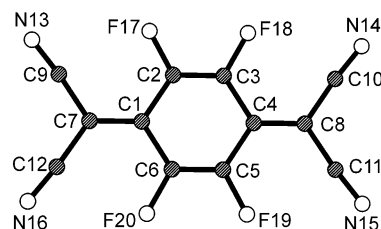


Figure 1. Atom labeling in TCNQ-F4 used in this work.

stable.^{13,14} Ab initio calculations on the cationic and anionic states of TCNQ and of TCNE were also performed by Zakrzewski et al.¹⁶ The vertical electron binding energy obtained for TCNQ, within the outer valence Green function (OVGF) method,^{17,18} was found to be 2.74 eV, and the energies of the $1^2B_{3u} \rightarrow 2^2B_{2g}$ transition obtained within the configuration interaction method with single excitations led to the conclusion that the 1^2B_{3u} anionic state of TCNQ is likely to be electronically stable with respect to the neutral species.¹⁶

In this contribution we focus our attention on a well-known electron acceptor molecule TCNQ-F4 (2,3,5,6-tetrafluoro-7,7,8,8-tetracyanoquinodimethane) shown in Figure 1. This system is of a great interest for material chemists because it plays the role of an electron acceptor in the formation of charge-transfer complexes.¹⁹ The TCNQ-F4[–] radical anion forms tight pairs in alkali metal salts such as [Na⁺/TCNQ-F4[–]] or [K⁺/TCNQ-F4[–]], even at room temperature.²⁰ In 1995 Sugimoto et al. reported the first observation of weak ferromagnetism in purely organic radical solids such as [Li⁺/TCNQ-F4[–]].²¹

Even though the applications of the TCNQ-F4 and its radical anion in various types of salts are widely known, little has been done on determining the properties of TCNQ-F4[–] itself. In

[†] Part of the special issue “Donald J. Kouri Festschrift”.

^{*} To whom correspondence should be addressed. E-mail: simons@chemistry.utah.edu.

[‡] University of Gdansk.

[§] University of Utah.

particular, to the best of our knowledge, the possibility of forming bound excited anionic states of TCNQ-F4 has not been described thus far. Therefore, we decided to take the first step in this direction by estimating the propensity of this common electron acceptor molecule to form electronically stable excited anionic states.

2. Methods

2.1. Treatment Employed. The properties of TCNQ-F4 in the lowest singlet state, as well as in the anionic doublet states were investigated at the self-consistent field (SCF) and the second-order Møller–Plesset perturbation (MP2) levels of theory. In addition, the vertical electron attachment energies of TCNQ-F4 were calculated at the fourth-order MP perturbation theory level. For the open-shell anions, we performed geometry optimizations and harmonic vibrational frequency calculations at the unrestricted Hartree–Fock (UHF) level. The values of S^2 in the UHF calculations were in the 0.773–0.992 range for doublet states; after annihilation they decreased to 0.750–0.805. For each optimized geometry of an anionic state, we undertook single-point MP2 calculations of the energy of the anion and its parent neutral species. In addition, MP4 estimates of the vertical electron binding energies of each anionic state were calculated at the minimum energy structure of the neutral TCNQ-F4.

In our work we use common definitions²² of the vertical electron detachment energy (VDE) and vertical electron attachment energy (VAE) characterizing the electron binding energy of the anion at its equilibrium structure and at the equilibrium geometry of the neutral parent, respectively. In particular, these two quantities are defined as follows:

$$\text{VDE} = E_{\text{N}}(\text{G}_{\text{A}}) - E_{\text{A}}(\text{G}_{\text{A}})$$

and

$$\text{VAE} = E_{\text{N}}(\text{G}_{\text{N}}) - E_{\text{A}}(\text{G}_{\text{N}})$$

where E_{N} and E_{A} indicate the total energy of the neutral and anionic species, respectively, calculated at the equilibrium geometry of the neutral (G_{N}) or anion (G_{A}).

We employed cc-pVDZ²³ basis sets with extra s and p sets of diffuse functions on each atom, as implemented in the original aug-cc-pVDZ basis. However, to make our calculations practical, we had to further limit the number of basis functions, so the d-symmetry *diffuse* functions included in the original aug-cc-pVDZ basis set were omitted in our work. We thus followed the example of Zakrzewski, Dolgounitcheva, and Ortiz who used the same approach to study a similar molecule: 7,7,8,8-tetracyanoquinodimethane (TCNQ).¹⁶ We label such basis sets aug(sp)-cc-pVDZ to indicate the lack of the d-symmetry basis functions in the diffuse set. The usefulness and relevance of employing that particular basis set is explained in the following section.

All calculations were performed with the GAUSSIAN98 program²⁴ on Intel Pentium IV, AMD Athlon computers and on a Compaq Sierra numerical server. The three-dimensional plots of molecular orbitals were generated with the MOLDEN program.²⁵

2.2. Basis Set Testing. To test the usefulness the aug(sp)-cc-pVDZ basis set we used to calculate the properties of the TCNQ-F4[−] anionic states, we compared, for TCNE, results obtained with this basis set to the results when the full aug-(sp)-cc-pVDZ basis set (i.e., aug-cc-pVDZ) was used. As described by the Ortiz group, the vertical electron affinity of

TCNE (tetracyanoethylene) was found to be 2.03, 2.02, and 2.04 eV with the aug(sp)-cc-pVDZ, aug-cc-pVDZ, and cc-pVTZ basis sets, respectively.¹⁶ Taking into account that TCNE is similar to TCNQ-F4 (i.e., it is a very strong electron acceptor supporting bound excited anionic states), we conclude that the vertical electron affinity obtained for this species with the aug-cc-pVDZ basis set and with the aug(sp)-cc-pVDZ basis are likely to be almost the same because the VEAs differ by only 0.01 eV (0.5%) for TCNE. We also tested that, for the TCNQ-F4[−] species studied in our work, the SCF vertical electron attachment energy (VAE) for the ground doublet B_{2g} anionic state decreases by only 0.08 eV when the aug(sp)-cc-pVDZ basis is replaced with the aug-cc-pVDZ basis set (this corresponds to ca. 2% of the total VAE).

Next we decided to test the ability of the SCF/aug(sp)-cc-pVDZ treatment to reproduce the ground-state neutral and anionic equilibrium geometries. We performed SCF/aug(sp)-cc-pVDZ geometry optimizations of the neutral TCNQ (tetracyanoquinodimethane) and its anionic daughter (in its ground electronic doublet B_{2g} state) because the TCNQ system is a very similar species and its properties are described in the literature. We found that (i) for the neutral singlet A_g state of TCNQ the SCF/aug(sp)-cc-pVDZ bond lengths differ by less than 0.025 Å from those obtained via crystallographic measurements,²⁶ (ii) for the neutral singlet A_g state of TCNQ the SCF/aug(sp)-cc-pVDZ valence angles differ by less than 0.4° from those obtained experimentally (X-ray),²⁶ (iii) for the ground doublet B_{2g} state of TCNQ[−] the SCF/aug(sp)-cc-pVDZ bond lengths differ by less than 0.010 Å from those obtained experimentally (X-ray),²⁷ and (iv) for the ground doublet B_{2g} state of TCNQ[−] the SCF/aug(sp)-cc-pVDZ valence angles differ by less than 0.8° from X-ray.²⁷

In addition, we compared an X-ray structure²⁸ of the neutral TCNQ-F4 to our SCF/aug(sp)-cc-pVDZ optimized ground-state geometry; see Table 1. We found that the differences in the bond lengths never exceed 0.04 Å and the largest shift is for the C–F bond (the corresponding X-ray estimated bond length is shorter by 0.032 Å than our value). As far as the valence angles are concerned, the differences never exceed 0.7° and the largest change we observe for the C–C–N angle (0.62°).

To test the ability of the SCF/aug(sp)-cc-pVDZ treatment to reproduce excited-state anionic equilibrium geometries, we calculated the SCF/aug(sp)-cc-pVDZ equilibrium geometry of the lowest excited doublet anionic state of TCNQ (possessing B_{3u} symmetry) and we compared our results to those reported by Skurski and Gutowski¹⁵ obtained at the CI/PM3 level. We did this because (i) an experimental doublet B_{3u} excited-state TCNQ[−] geometry is not available and (ii) the CI/PM3 treatment has proven useful in reproducing the ground and excited-state geometries of the TCNQ/TCNQ[−].¹⁵ We found that (i) for the lowest doublet excited B_{3u} state of TCNQ[−], the SCF/aug(sp)-cc-pVDZ bond lengths differ by less than 0.036 Å from those calculated at the CI/PM3 level¹⁵ and (ii) for the lowest doublet excited B_{3u} state of TCNQ[−] the SCF/aug(sp)-cc-pVDZ valence angles differ by less than 0.4° from those calculated at the CI/PM3 level.

To test the ability of the SCF/aug(sp)-cc-pVDZ treatment to reproduce ground-state neutral and anionic harmonic frequencies, we compared such calculated vibrational modes to the frequencies obtained experimentally and available in the literature.²⁹ We conclude that (i) the largest shift for the neutral TCNQ-F4 is 383 cm^{−1} for the stiffest b_{2u} symmetry mode (when *unscaled* SCF/aug(sp)-cc-pVDZ frequencies are used), (ii) the largest shift for the anionic TCNQ-F4 is 220 cm^{−1} for the stiffest

TABLE 1: Geometrical Parameters of Neutral TCNQ-F4 in Its Lowest Singlet State and TCNQ-F4⁻ in Its Ground Doublet ¹B_{2g} State and Excited ¹A_u, ¹A_g, and ²A States Calculated at the Hartree-Fock Level with the aug(sp)-cc-pVDZ Basis Sets^a

species state (symmetry)	bond lengths r (Å), valence angles α (deg), and dihedral angles θ (deg)														
neutral 1A_g (D_{2h})	r C ₁ C ₂	1.463	(1.436)	r C ₁ C ₇	1.351	(1.372)	r C ₂ C ₃	1.328	(1.334)	r C ₂ F ₁₇	1.306	(1.338)	r C ₇ C ₉	1.445	(1.435)
	r C ₃ N ₁₃	1.136	(1.142)												
	α C ₁ C ₇ C ₉	124.29	(124.12)	α C ₂ C ₁ C ₇	123.12	(123.53)	α C ₇ C ₃ N ₁₃	175.33	(175.82)	α F ₁₇ C ₂ C ₃	118.97	(118.90)			
	r C ₁ C ₂	1.422		r C ₁ C ₇	1.412		r C ₂ C ₃	1.354		r C ₂ F ₁₇	1.324		r C ₇ C ₉	1.430	
	r C ₃ N ₁₃	1.144													
anion 1^2B_g (D_{2h})	α C ₁ C ₇ C ₉	123.99		α C ₂ C ₁ C ₇	123.72		α C ₇ C ₃ N ₁₃	175.65		α F ₁₇ C ₂ C ₃	117.42				
	r C ₁ C ₂	1.391		r C ₁ C ₇	1.470		r C ₂ C ₃	1.376		r C ₂ F ₁₇	1.326		r C ₇ C ₉	1.402	
	r C ₃ N ₁₃	1.165													
	α C ₁ C ₇ C ₉	122.44		α C ₂ C ₁ C ₇	122.53		α C ₇ C ₃ N ₁₃	178.47		α F ₁₇ C ₂ C ₃	117.98				
	θ C ₁ C ₇ C ₃ N ₁₃	151.77		θ C ₂ C ₁ C ₇ C ₉	39.42		θ F ₁₇ C ₂ C ₃ C ₄	178.54							
anion 1^2A (2^2B_{3u}) (C_2)	r C ₁ C ₂	1.486		r C ₁ C ₆	1.486		r C ₁ C ₇	1.383		r C ₂ C ₃	1.312		r C ₂ F ₁₇	1.329	
	r C ₃ F ₁₈	1.327		r C ₇ C ₉	1.432		r C ₇ C ₁₂	1.432		r C ₉ N ₁₃	1.143		r C ₁₀ N ₁₄	1.144	
	α C ₁ C ₂ C ₃	111.81		α C ₁ C ₇ C ₉	122.21		α C ₁ C ₇ C ₁₂	122.23		α C ₂ C ₁ C ₇	122.84		α C ₂ C ₃ C ₄	111.92	
	α C ₆ C ₁ C ₇	122.96		α C ₇ C ₉ N ₁₃	178.79		α C ₇ C ₁₂ N ₁₆	178.91		α F ₁₇ C ₂ C ₃	126.14		α F ₁₈ C ₃ C ₂	126.12	
	θ C ₁ C ₂ C ₃ C ₄	0.08		θ C ₁ C ₇ C ₉ N ₁₃	149.65		θ C ₁ C ₇ C ₁₂ N ₁₆	48.46		θ C ₂ C ₁ C ₇ C ₉	51.65		θ C ₂ C ₁ C ₇ C ₉	2.12	
	θ C ₂ C ₁ C ₇ C ₁₂	2.61		θ C ₂ C ₃ C ₄ C ₈	55.64		θ C ₃ C ₂ C ₇	124.29		θ C ₃ C ₄ C ₈ C ₁₀	128.27		θ C ₃ C ₄ C ₈ C ₁₀	178.28	
	θ C ₆ C ₁ C ₇ C ₉	177.79		θ F ₁₇ C ₂ C ₁ C ₇	116.93		θ F ₁₇ C ₂ C ₃ C ₄	7.85		θ F ₁₈ C ₃ C ₂ C ₁	173.69		θ F ₁₈ C ₃ C ₄ C ₈	61.70	

^a Experimental parameters are given in parentheses.²⁸

b_{1u} symmetry mode (again, when unscaled SCF/aug(sp)-cc-pVDZ frequencies are used), (iii) the largest shift for the neutral TCNQ-F4 is 105 cm⁻¹ for the stiffest b_{2u} symmetry mode (with scaled SCF/aug(sp)-cc-pVDZ frequencies), and (iv) the largest shift for the anionic TCNQ-F4 is 38 cm⁻¹ for the stiffest b_{1u} symmetry mode (with scaled SCF/aug(sp)-cc-pVDZ frequencies). We employed the 0.8929 scaling factor commonly used to scale SCF frequencies (see ref 30), and we found significantly better agreement with the experimental results. Therefore, we decided to present *scaled* (by 0.8929) SCF vibrational frequencies for the species discussed in this work.

To test the ability of the SCF/aug(sp)-cc-pVDZ treatment to reproduce the excited-state anionic harmonic frequencies, we calculated the harmonic vibrational frequencies of the lowest excited doublet anionic state (²B_{3u}) of TCNQ (at the SCF level with the aug(sp)-cc-pVDZ basis sets) and we compared our results to those reported in ref 15 obtained at the CI/PM3 level. We did this because (i) the experimental doublet B_{3u} excited-state TCNQ⁻ frequencies are not available and (ii) the CI/PM3 treatment has proven useful in reproducing the ground- and excited-state frequencies of the TCNQ/TCNQ⁻ species (see ref 15). We found that the differences between the corresponding SCF/aug(sp)-cc-pVDZ and CI/PM3 harmonic vibrational frequencies are not larger than 120 cm⁻¹ (in worst cases), which corresponds to ca. 3–4%. Therefore, we conclude that the treatment we employed is suitable for estimating vibrational frequencies of TCNQ-F4⁻ in its excited states.

Finally, we tested the ability of the MP4/aug(sp)-cc-pVDZ treatment to reproduce electronic stabilities of the anions (in general). Again, we used the TCNQ/TCNQ⁻ system that is similar to TCNQ-F4/TCNQ-F4⁻ and for which the vertical electron affinity is known. For the ground doublet B_{2g} anionic state the experimental results available are 2.8 ± 0.1 eV^{31,32} and 2.84 ± 0.05 eV,³³ whereas the theoretical result by Zakrzewski et al. (calculated at the OVGF/aug(sp)-cc-pVDZ level) is 2.74 eV.¹⁶ Our result (which is the vertical electron detachment energy calculated at MP4/aug(sp)-cc-pVDZ level) is 2.915 eV, which is relatively close to the experimental results (in fact, it is almost in the range of the experimental error). Therefore, we conclude that the MP4/aug(sp)-cc-pVDZ treatment is suitable for calculating the electron binding energies of strongly bound anions (such as TCNQ-F4⁻).

3. Results

3.1. Neutral TCNQ-F4 and the Lowest (Ground) Doublet State of TCNQ-F4⁻. The lowest singlet ¹A_g (4b_{3u}²) state of the neutral TCNQ-F4 was found to have a minimum energy structure at *D*_{2h} symmetry (see Figure 2). The structural parameters characterizing this *D*_{2h} minimum are defined in Figure 1 and specified in Table 1. Because the orbital energy of the lowest unoccupied molecular orbital (LUMO) of b_{2g} symmetry is negative (−2.342 eV), one anticipates at least one electronically stable anionic state (in which the excess electron occupies the b_{2g} orbital leading to a 4b_{3u}²4b_{2g}¹ electronic configuration). Indeed, we found the ¹B_{2g} (4b_{3u}²4b_{2g}¹) anion to be both electronically and geometrically stable and to possess *D*_{2h} symmetry (see Figure 2). The geometry of the ¹B_{2g} anion is slightly different than that calculated for the neutral parent (¹A_g) primarily because of the bonding/antibonding pattern of the b_{2g} orbital that holds the extra electron (see Figure 3). In particular, the singly occupied b_{2g} orbital is characterized by C₁–C₂, C₁–C₆, C₃–C₄, and C₄–C₅ bonding interactions and C₁–C₇, C₄–C₈, and C₇(C₈)–N_{13,16}(N_{14,15}) antibonding interactions, which are consistent with the changes in the bond lengths

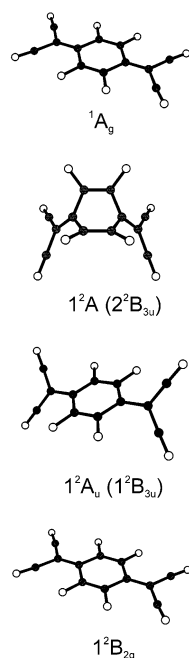


Figure 2. Equilibrium structures of the neutral TCNQ-F4 (top) and anionic TCNQ-F4[−] in its ground doublet 1^2B_{2g} state and excited 1^2A_u and 1^2A states calculated at the Hartree–Fock level with the aug(sp)-cc-pVDZ basis sets.

when the 1^2B_{2g} anion is formed. Indeed, the largest shortening in the bond length upon attachment of an excess electron is for the C_1 – C_2 bond (by 0.041 Å) and the largest elongation is observed for the C_1 – C_7 bond (by 0.061 Å); see Table 1. The changes of the valence angles upon excess electron attachment are relatively small, and we found the largest difference for the $C_2C_3F_{17}$ angle (+1.56°) whereas other differences do not exceed 1° (see Table 1).

To assist in possible experimental identification of the states of this anion, in Table 2 we give the *scaled* (by 0.8929) SCF/aug(sp)-pVDZ harmonic vibrational frequencies for the 1A_g neutral and 1^2B_{2g} anion (together with the frequencies calculated for three other excited anionic states that are described in further sections). As shown in Table 2, the frequencies of the stiff modes usually decrease upon electron attachment. In particular, this tendency manifests itself especially for b_{1u} , b_{2u} , b_{3g} , and a_g symmetry modes and the largest shifts we observe for ν_{31} (b_{3g}) (−205 cm^{-1}), ν_{49} (b_{2u}) (−204 cm^{-1}), ν_{40} (b_{1u}) (−168 cm^{-1}), and ν_{10} (a_g) (−162 cm^{-1}).

3.2. Excited Anionic States of TCNQ-F4. Because a primary goal was to investigate the stability of excited electronic states of anionic TCNQ-F4, we considered two paths leading to such anions. While studying both, we assumed the ground electronic state of the anion (i.e., the 1^2B_{2g} state, possessing $4b_{3u}^24b_{2g}^1$ configuration) to be the starting point. The states of the “first kind” are the result of promoting an electron from the singly occupied $4b_{2g}$ orbital to low-lying virtual orbitals. In particular, this leads to two *valence-excited* anionic states: a 1^2A_g state ($4b_{3u}^24b_{2g}^017a_g^1$) in which the LUMO+1 of the neutral is singly occupied, and a 2^2B_{3u} state ($4b_{3u}^24b_{2g}^05b_{3u}^1$) in which the LUMO+2 of the neutral is singly occupied. These states are called valence-excited because they are derived from the ground anionic state 1^2B_{2g} ($4b_{3u}^24b_{2g}^117a_g^05b_{3u}^0$) by exciting an electron from the valence b_{2g} orbital to one of the higher energy virtual orbitals.

Another possibility of forming an excited anionic state involves excitation of one of the electrons from a doubly

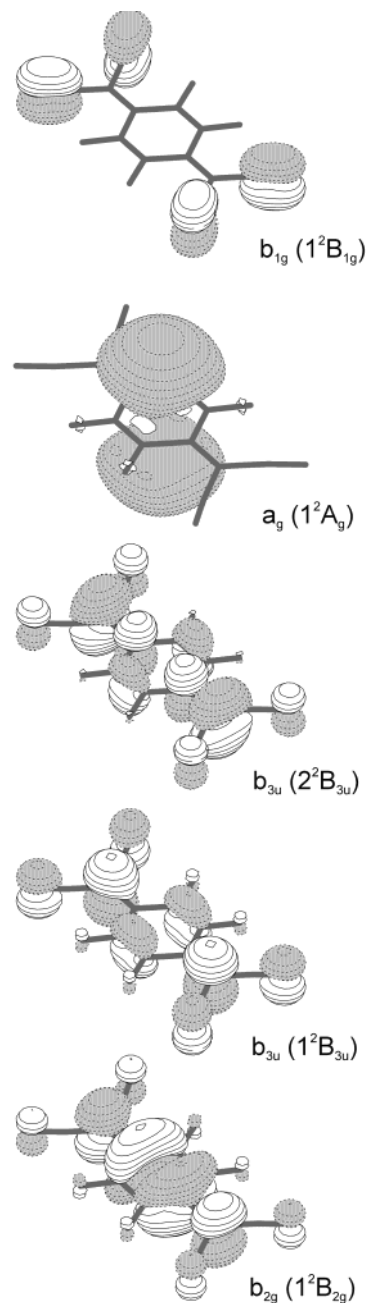


Figure 3. Singly occupied molecular orbitals in various doublet anionic states of TCNQ-F4 at the equilibrium D_{2h} geometry of the neutral species.

occupied orbital. In our case this led to two states: a 1^2B_{3u} state ($3b_{1g}^24b_{3u}^14b_{2g}^2$) and a 1^2B_{1g} state ($3b_{1g}^14b_{3u}^24b_{2g}^2$). We consider these as *core-excited* states because they were formed by promoting an electron in the ground 1^2B_{1g} state from a doubly occupied orbital (either $3b_{1g}$ or $4b_{3u}$) to the $4b_{2g}$ orbital (which is the LUMO in the neutral). This leads to a state in which the $4b_{2g}$ orbital is doubly occupied and one of the “core” orbitals (i.e., either $3b_{1g}$ or $4b_{3u}$) becomes singly occupied and thus determines the symmetry.

3.2.1. Excess Electron Binding by the Neutral TCNQ-F4 at Its Minimum-Energy Structure. First we consider the electronic stability of such excited anionic states at the D_{2h} minimum-energy structure of the parent neutral species. The calculated vertical electron binding energies at this geometry correspond to vertical electron attachment energies (VAEs) and describe the propensity of forming anionic states by the neutral TCNQ-F4 in its most stable conformation. Our MP4 results

TABLE 2: Scaled (by 0.8929) Harmonic Vibrational Frequencies (cm^{-1}) of TCNQ-F4 in the Lowest Singlet State and TCNQ-F4⁻ in the Low-Lying Doublet Electronic States Calculated at the Hartree-Fock Level with the aug(sp)-cc-pVDZ Basis Sets^a

1^1A_g				1^2B_{2g}				$1^2A(2^2B_{3u})$				$1^2A_u(1^2B_{3u})$			
$\nu_1(a_g)$	136	$\nu_{30}(b_{3g})$	1418	$\nu_1(a_g)$	138	$\nu_{30}(b_{3g})$	1502	$\nu_1(a)$	32	$\nu_{28}(a)$	2167	$\nu_1(a_g)$	39	$\nu_{28}(b_g)$	96
$\nu_2(a_g)$	289		(1498)	$\nu_2(a_g)$	290	$\nu_{31}(b_{3g})$	2115	$\nu_2(a)$	45	$\nu_{29}(b)$	38	$\nu_2(a_g)$	136	$\nu_{29}(b_g)$	188
	(298)	$\nu_{31}(b_{3g})$	2320		(299)	$\nu_{32}(b_{1u})$	156	$\nu_3(a)$	72	$\nu_{30}(b)$	52	$\nu_3(a_g)$	279	$\nu_{30}(b_g)$	254
$\nu_3(a_g)$	329		(2219)	$\nu_3(a_g)$	329	$\nu_{33}(b_{1u})$	307	$\nu_4(a)$	107	$\nu_{31}(b)$	95	$\nu_4(a_g)$	333	$\nu_{31}(b_g)$	381
	(343)	$\nu_{32}(b_{1u})$	153		(350)	$\nu_{34}(b_{1u})$	463	$\nu_5(a)$	116	$\nu_{32}(b)$	125	$\nu_5(a_g)$	415	$\nu_{32}(b_g)$	434
$\nu_4(a_g)$	454	$\nu_{33}(b_{1u})$	302	$\nu_4(a_g)$	471		(502)	$\nu_6(a)$	139	$\nu_{33}(b)$	173	$\nu_6(a_g)$	489	$\nu_{33}(b_g)$	506
	(484)	$\nu_{34}(b_{1u})$	479		(492)	$\nu_{35}(b_{1u})$	627	$\nu_7(a)$	200	$\nu_{34}(b)$	225	$\nu_7(a_g)$	502	$\nu_{34}(b_g)$	557
$\nu_5(a_g)$	620	$\nu_{35}(b_{1u})$	619	$\nu_5(a_g)$	629		(631)	$\nu_8(a)$	219	$\nu_{35}(b)$	244	$\nu_8(a_g)$	646	$\nu_{35}(b_g)$	747
	(620)		(618)		(636)	$\nu_{36}(b_{1u})$	772	$\nu_9(a)$	247	$\nu_{36}(b)$	299	$\nu_9(a_g)$	864	$\nu_{36}(b_g)$	766
$\nu_6(a_g)$	850	$\nu_{36}(b_{1u})$	780	$\nu_6(a_g)$	852		(789)	$\nu_{10}(a)$	377	$\nu_{37}(b)$	325	$\nu_{10}(a_g)$	1242	$\nu_{37}(b_g)$	1053
	(878)		(806)		(885)	$\nu_{37}(b_{1u})$	1105	$\nu_{11}(a)$	414	$\nu_{38}(b)$	392	$\nu_{11}(a_g)$	1424	$\nu_{38}(b_g)$	1103
$\nu_7(a_g)$	1257	$\nu_{37}(b_{1u})$	1093	$\nu_7(a_g)$	1244		(1143)	$\nu_{12}(a)$	438	$\nu_{39}(b)$	423	$\nu_{12}(a_g)$	1645	$\nu_{39}(b_g)$	1579
	(1273)		(1138)		(1269)	$\nu_{38}(b_{1u})$	1312	$\nu_{13}(a)$	448	$\nu_{40}(b)$	481	$\nu_{13}(a_g)$	2143	$\nu_{40}(b_g)$	2055
$\nu_8(a_g)$	1567	$\nu_{38}(b_{1u})$	1315	$\nu_8(a_g)$	1432		(1344)	$\nu_{14}(a)$	461	$\nu_{41}(b)$	535	$\nu_{14}(a_u)$	24	$\nu_{41}(b_u)$	38
	(1456)		(1347)		(1455)	$\nu_{39}(b_{1u})$	1448	$\nu_{15}(a)$	521	$\nu_{42}(b)$	596	$\nu_{15}(a_u)$	130	$\nu_{42}(b_u)$	70
$\nu_9(a_g)$	1728	$\nu_{39}(b_{1u})$	1607	$\nu_9(a_g)$	1664		(1500)	$\nu_{16}(a)$	561	$\nu_{43}(b)$	605	$\nu_{16}(a_u)$	151	$\nu_{43}(b_u)$	154
	(1665)		(1551)		(1655)	$\nu_{40}(b_{1u})$	2155	$\nu_{17}(a)$	595	$\nu_{44}(b)$	696	$\nu_{17}(a_u)$	263	$\nu_{44}(b_u)$	241
$\nu_{10}(a_g)$	2322	$\nu_{40}(b_{1u})$	2323	$\nu_{10}(a_g)$	2160		(2194)	$\nu_{18}(a)$	602	$\nu_{45}(b)$	804	$\nu_{18}(a_u)$	303	$\nu_{45}(b_u)$	304
	(2227)		(2228)		(2221)	$\nu_{41}(b_{2u})$	96	$\nu_{19}(a)$	746	$\nu_{46}(b)$	852	$\nu_{19}(a_u)$	469	$\nu_{46}(b_u)$	495
$\nu_{11}(a_u)$	43	$\nu_{41}(b_{2u})$	102	$\nu_{11}(a_u)$	21	$\nu_{42}(b_{2u})$	246	$\nu_{20}(a)$	825	$\nu_{47}(b)$	1005	$\nu_{20}(a_u)$	499	$\nu_{47}(b_u)$	554
$\nu_{12}(a_u)$	125	$\nu_{42}(b_{2u})$	251	$\nu_{12}(a_u)$	127		(261)	$\nu_{21}(a)$	1032	$\nu_{48}(b)$	1143	$\nu_{21}(a_u)$	639	$\nu_{48}(b_u)$	679
$\nu_{13}(a_u)$	421	$\nu_{43}(b_{2u})$	322	$\nu_{13}(a_u)$	441	$\nu_{43}(b_{2u})$	321	$\nu_{22}(a)$	1138	$\nu_{49}(b)$	1170	$\nu_{22}(a_u)$	671	$\nu_{49}(b_u)$	771
$\nu_{14}(a_u)$	635		(257)	$\nu_{14}(a_u)$	644	$\nu_{44}(b_{2u})$	479	$\nu_{23}(a)$	1154	$\nu_{50}(b)$	1276	$\nu_{23}(a_u)$	1121	$\nu_{50}(b_u)$	943
$\nu_{15}(b_{1g})$	50	$\nu_{44}(b_{2u})$	465	$\nu_{15}(b_{1g})$	24	$\nu_{45}(b_{2u})$	938	$\nu_{24}(a)$	1316	$\nu_{51}(b)$	1309	$\nu_{24}(a_u)$	1300	$\nu_{51}(b_u)$	1095
$\nu_{16}(b_{1g})$	372		(330)	$\nu_{16}(b_{1g})$	397		(967)	$\nu_{25}(a)$	1442	$\nu_{52}(b)$	1714	$\nu_{25}(a_u)$	1476	$\nu_{52}(b_u)$	1155
$\nu_{17}(b_{1g})$	454	$\nu_{45}(b_{2u})$	945	$\nu_{17}(b_{1g})$	448	$\nu_{46}(b_{2u})$	1141	$\nu_{26}(a)$	1564	$\nu_{53}(b)$	2144	$\nu_{26}(a_u)$	2252	$\nu_{53}(b_u)$	1471
$\nu_{18}(b_{2g})$	78	$\nu_{46}(b_{2u})$	1154	$\nu_{18}(b_{2g})$	92		(1199)	$\nu_{27}(a)$	2143	$\nu_{54}(b)$	2156	$\nu_{27}(b_g)$	82	$\nu_{54}(b_u)$	2213
$\nu_{19}(b_{2g})$	211		(976)	$\nu_{19}(b_{2g})$	212	$\nu_{47}(b_{2u})$	1246								
$\nu_{20}(b_{2g})$	432	$\nu_{47}(b_{2u})$	1372	$\nu_{20}(b_{2g})$	395	$\nu_{48}(b_{2u})$	1531								
$\nu_{21}(b_{2g})$	626		(1394)	$\nu_{21}(b_{2g})$	561		(1536)								
$\nu_{22}(b_{2g})$	721	$\nu_{48}(b_{2u})$	1673	$\nu_{22}(b_{2g})$	736	$\nu_{49}(b_{2u})$	2115								
$\nu_{23}(b_{3g})$	152		(1598)	$\nu_{23}(b_{3g})$	146		(2172)								
$\nu_{24}(b_{3g})$	239	$\nu_{49}(b_{2u})$	2319	$\nu_{24}(b_{3g})$	232	$\nu_{50}(b_{3u})$	37								
$\nu_{25}(b_{3g})$	400		(2214)	$\nu_{25}(b_{3g})$	423	$\nu_{51}(b_{3u})$	164								
$\nu_{26}(b_{3g})$	452	$\nu_{50}(b_{3u})$	22	$\nu_{26}(b_{3g})$	467	$\nu_{52}(b_{3u})$	249								
$\nu_{27}(b_{3g})$	753	$\nu_{51}(b_{3u})$	159	$\nu_{27}(b_{3g})$	750	$\nu_{53}(b_{3u})$	547								
$\nu_{28}(b_{3g})$	1098	$\nu_{52}(b_{3u})$	257	$\nu_{28}(b_{3g})$	1080	$\nu_{54}(b_{3u})$	662								
$\nu_{29}(b_{3g})$	1153	$\nu_{53}(b_{3u})$	587	$\nu_{29}(b_{3g})$	1143										
	(1193)	$\nu_{54}(b_{3u})$	721												

^a Experimental frequencies are given in parentheses.²⁹**TABLE 3: Vertical (at the Neutral’s Equilibrium Geometry) Electron Attachment Energies (VAE, eV) of TCNQ-F4 Corresponding to the Ground and Various Excited States of the Anion Calculated at the MP2, and MP4 Levels with the aug(sp)-cc-pVDZ Basis Sets**

state (configuration)	description	VAE ^{MP4}	VAE ^{MP2}
$1^2B_{1g}(3b_{1g}^14b_{3u}^24b_{2g}^2)$	core-excited	<0	<0
$1^2A_g(4b_{3u}^24b_{2g}^017a_g^1)$	externally exc	0.072	0.038
$2^2B_{3u}(4b_{3u}^24b_{2g}^05b_{3u}^1)$	externally exc	0.244	0.419
$1^2B_{3u}(3b_{1g}^24b_{3u}^14b_{2g}^2)$	core-excited	0.822	1.150
$1^2B_{2g}(4b_{3u}^24b_{2g}^1)$	ground	2.893	3.294

indicate that four stable anionic states can be created (see Table 3): (i) the ground electronic state of the anion $1^2B_{2g}(4b_{3u}^24b_{2g}^1)$ whose VAE is 2.893 eV; (ii) the core-excited 1^2B_{3u} state ($3b_{1g}^24b_{3u}^14b_{2g}^2$) with vertical electron attachment energy of 0.822 eV; (iii) the valence-excited 2^2B_{3u} state ($4b_{3u}^24b_{2g}^05b_{3u}^1$) whose VAE = 0.244 eV; (iv) the valence-excited 1^2A_g state ($4b_{3u}^24b_{2g}^017a_g^1$) whose VAE is small but positive (0.072 eV). The core-excited 1^2B_{1g} state ($3b_{1g}^14b_{3u}^24b_{2g}^2$) as well as the other (higher) valence-excited anionic states (such as 1^2B_{1u}) were found to be unstable (at the MP4 level) with respect to electron loss.

It should also be noted that the corresponding MP2 vertical electron attachment energies given in Table 3 are larger than those obtained at the MP4 level for each state but 1^2A_g . In particular, the VAE values calculated at the MP2 level differ

by +0.401, +0.328, +0.175, and -0.034 eV, for 1^2B_{2g} , 1^2B_{3u} , 2^2B_{3u} , and 1^2A_g , respectively. Because the VAEs seem somewhat overestimated when calculated at the MP2 level with respect to those obtained at the fourth-order MP perturbation theory, we believe that there should be no other anionic states electronically stable except those that have proven stable at the MP4 level.

3.2.2. Valence-Excited Anionic States of TCNQ-F4 and Their Geometric Stability. Our search for electronically stable anionic states at the D_{2h} minimum energy structure of the neutral TCNQ-F4 led to the conclusion that there are four stable doublet states of TCNQ-F4⁻. The 1^2B_{2g} state is the ground state of the anion, whereas two states of B_{3u} symmetry and one state of A_g symmetry are higher in energy, although they remain electronically stable with respect to the neutral molecule. As stated in section 3.1, the minimum-energy structure for the ground state of the anion, 1^2B_{2g} , corresponds to D_{2h} symmetry. This state lies significantly lower in energy (by 2.893 eV) than the ground singlet A_g state of the neutral molecule. The description of the geometrical parameters and harmonic vibrational frequencies characterizing the doublet B_{2g} state were given in section 3.1, so now we discuss the excited anionic states only, for which the situation is much more complicated.

Let us begin with the valence-excited doublet B_{3u} anionic states (i.e., 2^2B_{3u}) and A_g (i.e., 1^2A_g). Even though the vertical

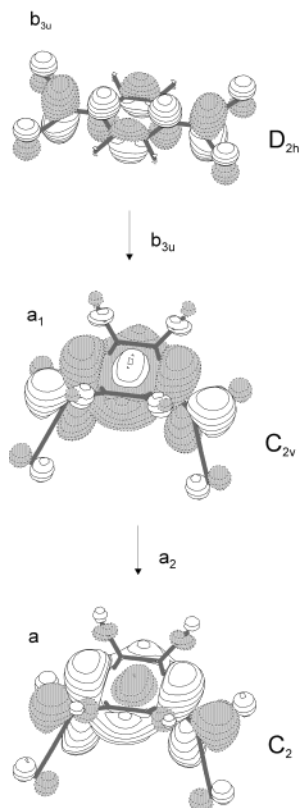


Figure 4. “Evolution” of the singly occupied molecular orbital in the 2^2B_{3u} anionic state caused by second-order Jahn–Teller effects leading to the 1^2A anionic state.

attachment energies calculated for these two states are positive (see the preceding section 3.2.1. and Table 3), we found these anions to be geometrically unstable at D_{2h} symmetry.

A. Valence-Excited 2^2B_{3u} State of TCNQ-F4 $^-$. In particular, for the 2^2B_{3u} state, the minimum-energy structure preserving D_{2h} symmetry possesses an imaginary frequency of b_{3u} symmetry. The fact that another valence-excited state (1^2A_g) state is close in energy (see Table 3) causes second-order Jahn–Teller instability, which manifests itself as negative curvature along the b_{3u} symmetry mode. We then proceeded in our search for a geometrically stable anionic state by deforming the planar D_{2h} structure of the 2^2B_{3u} anion along the imaginary mode of b_{3u} symmetry (see Figure 4). This led to lowering of the symmetry (to C_{2v} symmetry) of the molecule and the singly occupied b_{3u} orbital became an a_1 orbital in the final C_{2v} point group. As can be seen in Figure 4, the molecule became nonplanar and especially the $-C(CN)_2$ groups bent with respect to the carbon ring. Although the geometry optimization procedure led to a stationary point on the potential energy surface, vibrational analysis indicated an imaginary frequency of a_2 symmetry. We consequently deformed the geometry along that negative curvature, subsequently achieving a C_2 symmetry structure. For this symmetry, the a_1 singly occupied orbital became an a -symmetry orbital (because it is even with respect to the rotation around the C_2 axis). Geometry optimization performed in the C_2 group led eventually to a true minimum on the potential energy surface and the corresponding harmonic vibrational frequencies for this final doublet A state (termed 1^2A) are given in Table 2.

The equilibrium geometry of this 1^2A state is far from planarity. Instead, the structure is strongly bent (see Figure 2 and the right bottom structure in Figure 4). Both $-C(CN)_2$ groups point in the same direction whereas all four fluorine

TABLE 4: Vertical Electron Detachment Energies (VDE, eV) of TCNQ-F4 $^-$ Corresponding to the Ground and Various Excited States of the Anion Calculated at the MP2 Level with the aug(sp)-cc-pVDZ Basis Sets

Final state (original state)	description	VDE ^{MP2}
1^2B_1 (1^2B_{1g})	core-excited	<0
1^2A (2^2B_{3u})	externally exc.	2.721
1^2A_u (1^2B_{3u})	core-excited	<0
1^2B_{2g} (1^2B_{2g})	ground	3.665

atoms are directed to the opposite side of the carbon ring (see Table 1 for precise values of geometrical parameters). The vertical electron binding energy of this 1^2A state increases when the equilibrium geometry for this anion is achieved, and our best estimate of the VDE at the MP2 level is 2.721 eV; see Table 4. Therefore, we conclude that the 2^2B_{3u} anionic state, characterized by $VAE^{MP4} = 0.244$ eV at the equilibrium D_{2h} geometry of the neutral TCNQ-F4, evolves to a much more electronically stable species at its minimum-energy structure, and the driving force of this geometry deformation is the second-order Jahn–Teller coupling to another excited state of A_g symmetry.

B. Valence-Excited 1^2A_g State of TCNQ-F4 $^-$. The other valence-excited anionic doublet state (1^2A_g) would be expected to increase in energy while the geometry of this species is deformed along the distortion mode that couples it to the 2^2B_{3u} state. This is because the 2^2B_{3u} and 1^2A_g states avoid each other, and the former’s energy decreases whereas the latter’s energy increase along the distortion in the coupling mode takes place. Unfortunately, unlike for the 2^2B_{3u} state, we were not able to follow the 1^2A_g state that moves uphill in energy because it evolves into a doublet A_1 state (in the C_{2v} symmetry group) as does the 2^2B_{3u} state. As a consequence, our attempts to investigate the evolution of that state failed because the SCF procedure we used always converged to the lowest 2^2A_1 state (corresponding to 2^2B_{3u}), which is the lowest energy state of that symmetry. We conclude that a multiconfigurational treatment would be necessary if one wants to describe the evolution of the 1^2A_g state. However, employing such a treatment for the open-shell system containing twenty heavy atoms (as TCNQ-F4 does) with the aug(sp)-cc-pVDZ basis sets was not practical for us with the computer resources at hand, so we were unable to further explore this particular state.

3.2.3. Core-Excited Anionic States of TCNQ-F4. In this section we discuss the core-excited doublet anionic states of 1^2B_{3u} and 1^2B_{1g} symmetry. As was the case for the two bound valence-excited states described in the previous section, we found these anions to be geometrically unstable at D_{2h} symmetry.

A. Core-Excited 1^2B_{3u} State of TCNQ-F4 $^-$. Although the 1^2B_{3u} state is characterized by a relatively large value of the vertical electron binding energy calculated for the minimum-energy structure of the neutral ($VDE^{MP4} = 0.822$ eV), its minimum-energy structure preserving D_{2h} symmetry possesses an imaginary frequency of b_{1g} symmetry. We proceeded in our search for a geometrically stable anionic state by deforming the planar D_{2h} structure of the 1^2B_{3u} anion along the imaginary mode of b_{1g} symmetry (see Figure 5). This led to the lowering of the symmetry (C_{2h} symmetry was achieved) of the molecule and the singly occupied b_{3u} orbital became an a_u orbital in the final C_{2h} point group. The geometry optimization performed in the C_{2h} group led to a true minimum on the potential energy surface, and the corresponding harmonic vibrational frequencies for this final doublet A_u state (termed 1^2A_u) are given in Table 2.

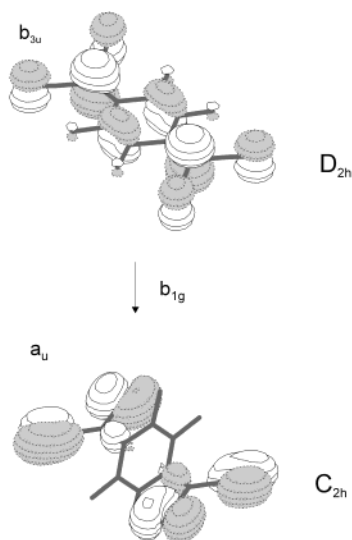


Figure 5. “Evolution” of the singly occupied molecular orbital in the 1^2B_{3u} anionic state leading to the 1^2A_u anionic state.

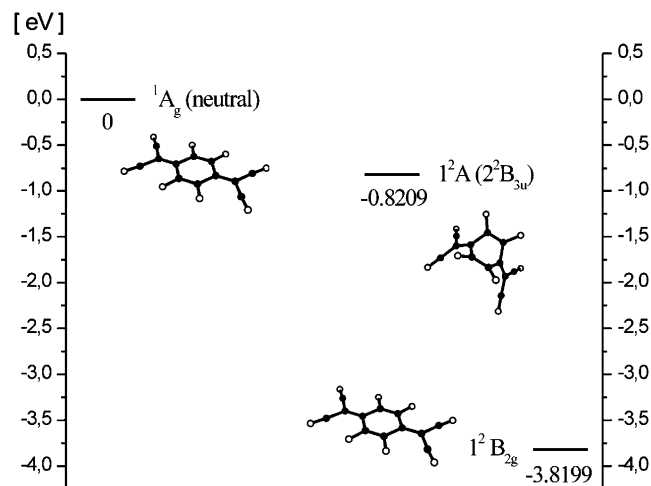


Figure 6. Relative SCF energies (eV) of three electronically stable anionic states of TCNQ-F4 calculated at their SCF equilibrium geometries (the zero of energy is taken to be the total electronic energy of the neutral TCNQ-F4 at its minimum energy structure).

The equilibrium geometry achieved for the anion in its 1^2A_u state is depicted in Figure 2, and the geometrical parameters are collected in Table 1. It can be seen that the 1^2A_u anionic structure differs from the structures obtained for other anionic states primarily because the two $-C(CN)_2$ groups remain in one plane although they are twisted with respect to the carbon ring.

Although the SCF vertical electron binding energy of the 1^2A_u state increases when the equilibrium geometry for this anion is achieved, we verified that the inclusion of electron correlation renders this anion electronically unstable (i.e., the calculated value of the VDE at the MP2 level is negative). Therefore, we conclude that the core-excited 1^2B_{3u} anionic state, although electronically stable at the minimum energy structure of the neutral species, is unstable when the geometry is relaxed and electron correlation is taken into account. We believe more sophisticated calculations (such as geometry optimization at either the configuration-interaction or multireference SCF level) should be performed to achieve the final judgment considering the electronic stability of this state.

B. Other Core-Excited States of TCNQ-F4[−]. Among other possible core-excited states of TCNQ-F4[−], we focused our

attention primarily on the 1^2B_{1g} state possessing $3b_{1g}^14b_{3u}^24b_{2g}^2$ electronic configuration. However, we verified that this state is electronically unstable with respect to the neutral molecule at its D_{2h} minimum energy structure. Even though we spent considerable effort searching for a geometry at which the 1^2B_{1g} state would be electronically stable, we were not able to find any. In particular, we verified that the 1^2B_{1g} state lowers its energy if deformed along the a_u imaginary mode (achieving D_2 symmetry) but the energy decrease is not large enough to render this anion electronically stable. Moreover, our attempts to form other bound core-excited states of the anion failed; thus we are reasonably confident the 1^2B_{3u} (becoming eventually 1^2A_u) core-excited state is the only such state that is stable with respect to the neutral parent molecule, although its electronic stability should be confirmed by higher-level calculations (see section 3.2.3.A).

4. Summary

The ground and bound excited anionic states of the common electron acceptor TCNQ-F4 were studied at the SCF, MP2, and MP4 levels of theory with the one-electron aug(sp)-cc-pVDZ basis sets. On the basis of our calculations we conclude that

The ground electronic state of TCNQ-F4[−] is the 1^2B_{2g} state ($4b_{3u}^24b_{2g}^1$) whose MP4 vertical electron attachment energy is 2.893 eV. This state possesses its minimum for D_{2h} symmetry.

There are three excited anionic states of TCNQ-F4 that are vertically electronically stable at the D_{2h} minimum energy structure of the neutral system. These are the core-excited 1^2B_{3u} state ($3b_{1g}^24b_{3u}^14b_{2g}^2$), the valence-excited 2^2B_{3u} state ($4b_{3u}^24b_{2g}^05b_{3u}^1$), and the valence-excited 1^2A_g state ($4b_{3u}^24b_{2g}^017a_g^1$), whose MP4 vertical electron attachment energies are 0.822, 0.244, and 0.072 eV, respectively (see also Figure 6 where the SCF electron affinities of these anions are depicted).

Although the ground anionic 1^2B_{2g} state is geometrically stable at the D_{2h} symmetry, the other excited states are second-order Jahn–Teller unstable, which leads to the symmetry lowering for these species. As a consequence, the geometries of two 2^2B_{3u} and 1^2A_g valence-excited states deform and the former achieves a bent C_2 -symmetry minimum-energy structure with a vertical electron detachment energy of the resulting 1^2A state estimated to be 2.721 eV at the MP2 level. The energy of the 1^2A_g state could not be followed to its minimum-energy structure because of variational collapse. The structure of the core-excited 1^2B_{3u} anion deforms to C_{2h} symmetry, but this state was found to be electronically unstable when electron correlation is taken into account at the MP2 level. We believe that more sophisticated calculations are necessary to test the electronic stability of this particular state.

Acknowledgment. This work was supported by NSF Grant 9982420 to J.S. and the Polish State Committee for Scientific Research (KBN) Grant No. DS/8371-4-0137-2 to P.S.. The computer time provided by the Center for High Performance Computing at the University of Utah and the Academic Computer Center in Gdansk (TASK) is also gratefully acknowledged.

References and Notes

- (1) Feldman, D. *Chem. Phys. Lett.* **1977**, *47*, 338.
- (2) Lineberger, W. C.; Patterson, T. A. *Chem. Phys. Lett.* **1972**, *13*, 40.
- (3) Nimlos, M. R.; Harding, L. B.; Ellison, G. B. *J. Chem. Phys.* **1987**, *87*, 5116.

- (4) Gutowski, M.; Skurski, P. *Recent Res. Dev. Phys. Chem.* **1999**, *3*, 245.
- (5) Gutsev, G. L.; Bartlett, R. J. *J. Chem. Phys.* **1996**, *105*, 8785.
- (6) Skurski, P.; Gutowski, M.; Simons, J. *J. Chem. Phys.* **1999**, *110*, 274.
- (7) Skurski, P.; Gutowski, M.; Simons, J. *J. Phys. Chem. A* **1999**, *103*, 625.
- (8) Smith, D. M. A.; Smets, J.; Elkadi, Y.; Adamowicz, L. *J. Chem. Phys.* **1997**, *107*, 5788.
- (9) Jordan, K. D.; Luken, W. J. *J. Chem. Phys.* **1976**, *64*, 2760.
- (10) Gutowski, M.; Simons, J. *J. Chem. Phys.* **1994**, *100*, 1308.
- (11) Gutowski, M.; Simons, J. *J. Chem. Phys.* **1994**, *101*, 4867.
- (12) Gutowski, M.; Simons, J. *J. Phys. Chem.* **1994**, *98*, 8326.
- (13) Brinkman, E. A.; Günther, E.; Brauman, J. I. *J. Chem. Phys.* **1991**, *95*, 6185.
- (14) Brinkman, E. A.; Günther, E.; Schafer, O.; Brauman, J. I. *J. Chem. Phys.* **1994**, *100*, 1840.
- (15) Skurski, P.; Gutowski, M. *J. Mol. Struct. (THEOCHEM)* **2000**, *531*, 339.
- (16) Zakrzewski, V. G.; Dolgounitcheva, O.; Ortiz, J. V. *J. Chem. Phys.* **1996**, *105*, 5872.
- (17) Ortiz, J. V. *J. Chem. Phys.* **1988**, *89*, 6348.
- (18) Cederbaum, L. S. *J. Phys. B* **1975**, *8*, 290.
- (19) Wheland, R. C.; Martin, E. L. *J. Org. Chem.* **1975**, *40*, 3101.
- (20) Jones, M. T.; Maruo, T.; Jansen, S.; Roble, J.; Ratajczak, R. D. *Mol. Cryst. Liq. Cryst.* **1986**, *134*, 21.
- (21) Sugimoto, T.; Tsujii, M.; Matsuura, H.; Hosoi, N. *Chem. Phys. Lett.* **1995**, *235*, 183.
- (22) Kalcher, J.; Sax, A. F. *Chem. Rev.* **1994**, *94*, 2291.
- (23) Kendall, R. A.; Dunning, Jr., T. H.; Harrison, R. J. *J. Chem. Phys.* **1992**, *96*, 6796.
- (24) Frisch, M. J.; Trucks, G. W.; Schlegel, H. B.; Scuseria, G. E.; Robb, M. A.; Cheeseman, J. R.; Zakrzewski, V. G.; Montgomery, J. A., Jr.; Stratmann, R. E.; Burant, J. C.; Dapprich, S.; Millam, J. M.; Daniels, A. D.; Kudin, K. N.; Strain, M. C.; Farkas, O.; Tomasi, J.; Barone, V.; Cossi, M.; Cammi, R.; Mennucci, B.; Pomelli, C.; Adamo, C.; Clifford, S.; Ochterski, J.; Petersson, G. A.; Ayala, P. Y.; Cui, Q.; Morokuma, K.; Malick, D. K.; Rabuck, A. D.; Raghavachari, K.; Foresman, J. B.; Cioslowski, J.; Ortiz, J. V.; Stefanov, B. B.; Liu, G.; Liashenko, A.; Piskorz, P.; Komaromi, I.; Gomperts, R.; Martin, R. L.; Fox, D. J.; Keith, T.; Al-Laham, M. A.; Peng, C. Y.; Nanayakkara, A.; Gonzalez, C.; Challacombe, M.; Gill, P. M. W.; Johnson, B. G.; Chen, W.; Wong, M. W.; Andres, J. L.; Head-Gordon, M.; Replogle, E. S.; Pople, J. A. *Gaussian 98*, revision A.7; Gaussian, Inc.: Pittsburgh, PA, 1998.
- (25) Schaftenaar, G.; Noordik, J. H. MOLDEN: a pre- and postprocessing program for molecular and electronic structures. *J. Comput.-Aided Mol. Design* **2000**, *14*, 123.
- (26) Long, R. E.; Sparks, R. A.; Trueblood, K. N. *Acta Crystallogr.* **1965**, *18*, 932.
- (27) Hoekstra, A.; Spoelder, T.; Vos, A. *Acta Crystallogr.* **1972**, *B 28*, 14.
- (28) Emge, T. J.; Maxfield, M.; Cowan, D. O.; Kistenmacher, T. J. *Mol. Cryst. Liq. Cryst.* **1981**, *65*, 161.
- (29) Meneghetti, M.; Pecile, C. *J. Chem. Phys.* **1986**, *84*, 4149.
- (30) Frisch, M. J.; Frisch, E.; Foresman, J. B. *Gaussian94 User's Reference*; Gaussian, Inc.: Pittsburgh, PA, 1995 (ISBN: 0-9636769-1-1).
- (31) Klotz, C. E.; Compton, R. N.; Raaen, V. F. *J. Chem. Phys.* **1974**, *60*, 1177.
- (32) Compton, R. N.; Cooper, C. D. *J. Chem. Phys.* **1977**, *66*, 4325.
- (33) Chen, E. C. M.; Wentworth, W. E. *J. Chem. Phys.* **1975**, *63*, 3188.